文章编号：0258-8013 (2010) 15-0001-09 中图分类号：TM 351 文献标志码：A 学科分类号：470·40

电压源换流器高压直流输电的控制策略及其参数优化

郭春义，赵成勇

(电力系统保护与动态安全监控教育部重点实验室(华北电力大学)，北京市 昌平区 102206)

Novel Control Strategy for Voltage Source Converter Based HVDC and Controller Parameters Optimization

GUO Chun-yi, ZHAO Cheng-yong

(Key Laboratory of Power System Protection and Dynamic Security Monitoring and Control (North China Electric Power University), Ministry of Education, Changping District, Beijing 102206, China)

ABSTRACT: This paper proposes a novel control strategy for voltage source converter based high voltage direct current (VSC-HVDC). Based on its steady state model, a series of mathematical analysis expressions for power delivery were deduced using the coordinate conversion and variables substitution in terms of the original equations. The corresponding power controllers were designed using the PI controller and the nonlinear inverse system. Based on the designed strategy, the transmission limits of the active and reactive power were deduced. According to the circle characteristics of operation represented, it was theoretically proved that the control strategy could independently control the active and reactive power. Hooke-Jeeves algorithm was adopted to optimize the PI parameters of the proposed controllers for VSC-HVDC system. Simulation results obtained by using PSCAD/EMTDC show that better operation characteristics can be achieved with the support of optimized PI parameters. Moreover, the proposed controllers can independently control the active and reactive power with high response speed, desirable stability and strong robustness.

KEY WORDS: voltage source converter based on high voltage direct current (VSC-HVDC); control strategy; coordinate conversion; variables substitution; Hooke-Jeeves algorithm; parameters optimization

摘要：提出一种电压源换流器高压直流输电(voltage source converter based on high voltage direct current，VSC-HVDC)的新型控制策略。基于 VSC-HVDC 的稳态模型，通过坐标变换和变量代换推导出一组功率传输方程。结合 PI 控制器和非线性逆系统的思想设计了相应的控制器，并推导出在该控制器下 VSC-HVDC 的有功功率和无功功率的传输极限。从圆特性出发，在理论上证明所设计的控制器可以实现有功功率和无功功率的完全独立控制。采用 Hooke-Jeeves 算法对控制器的参数进行了优化。PSCAC/EMTDC 下的仿真结果表明：采用优化后的 PI 参数，系统性能得到很大改善；而且所设计的控制器可以实现有功功率和无功功率的独立控制，并具有快速的响应速度、良好的稳定性和较好的鲁棒性。

关键词：电压源换流器高压直流输电；控制策略；坐标变换；变量代换；Hooke-Jeeves 算法；参数优化

0 INTRODUCTION

The (voltage source converter based on high voltage direct current) VSC-HVDC uses pulse width modulation (PWM) with a relatively high switching frequency, which makes it possible to generate an AC output voltage with any desired phase angle or amplitude instantly [1-2]. A number of potential advantages of the VSC-HVDC are reported in the literature. For example, the VSC-HVDC system enables fast control of active and reactive power independently of each other [3-4]. It allows reactive power support to an area, if needed, independently of the active power transmitted, provided that the rating of the converter can handle the total apparent power.

基金项目：国家自然科学基金项目(50577018)；中央高校基本科研业务费专项资金资助项目(09QX62)。

Project Supported by National Science Foundation of China (50577018); Project Supported by Chinese Universities Scientific Fund (09QX62).

Moreover, active power flow can be quickly reversed, which is a desirable feature since it enables short-term transactions in electric power markets [5]. In addition, the VSC-HVDC system can feed power into passive networks with no local power generation [6-9].

Each converter station is composed of a VSC. The amplitude and phase angle of the converter AC output voltage can be controlled simultaneously to achieve a rapid, independent control of active and reactive power in all four quadrants. The control of both active and reactive power is bi-directional and continuous across the operating range. For active power balance, one of the converters operates on constant DC voltage control and the other converter operates on constant active power control. When DC line power is zero, the two converters can be considered as independent STATCOMs.

However, VSC is a double-input and double-output coupled nonlinear control object when it is connected to an active AC network [10]. The double-input refers to the phase angle δ and modulation index m of PWM, and the double-output refers to the reactive power output Q and the active power output P or the DC voltage U_d of the VSC. Due to the influence of the couple-relationship between controlling and controlled variables, it is difficult to control the active and reactive power independently, and enable the system to perform well. Therefore, it is necessary to develop a mathematical model for VSC-HVDC to determine the relationship between the two controlling and the two controlled variables, and fulfill the requirements of controlling active and reactive power independently.

At present, a lot of researches [11-15] have been done to study the control algorithms of the VSC-HVDC system, e.g. decoupled controllers based on dq reference frame, direct analysis expression method, nonlinear controller, etc. Also, many controller parameters optimization means are presented [16-18] for VSC-HVDC, such as genetic algorithm, simplex optimal algorithm, optimal and coordinate control scheme, etc. In this paper, a power control strategy is proposed based on the steady state model of VSC by the methods of the coordinate conversion and variables substitution, which can independently control the active and reactive power completely according to the circle characteristic of operation. The limitation of active and reactive power based on the strategy designed is deduced. Moreover，Hooke-Jeeves algorithm is adopted to optimize the PI parameters of proposed controllers. Compared with other optimization algorithms, Hooke-Jeeves algorithm owns particular advantages. Case studies are carried out with the help of PSCAD/EMTDC software so as to testify the control strategy designed and the optimization algorithm presented. The simulation results demonstrate that the controllers proposed with optimized parameters have high response speed, desirable stability, and strong robustness.

1 MODELING of VSC-HVDC

1.1 Steady State Model of VSC Based HVDC

The steady state model [19] of a VSC station linked to an active AC network is shown in Fig.1, where U_s is the root mean square (RMS) value of AC system voltage, U_c is the RMS value of the fundamental frequency component of the VSC output voltage, δ is the phase angle difference between $\dot{U}_s$ and $\dot{U}_c$, L is the equivalent inductance of converter reactor, R is the equivalent resistance of VSC's power loss, P_s and Q_s are the active and reactive power that the AC system provides, P_c and Q_c are the active and reactive power the VSC absorbs.

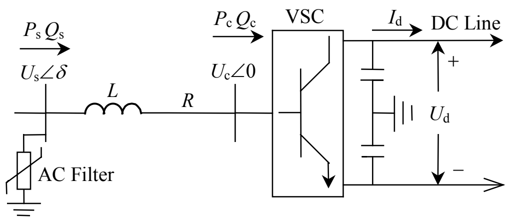

图 1 VSC-HVDC 的稳态模型

Fig. 1 Steady state model of VSC-HVDC

Let $X=\omega L$, $\alpha=\arctan(R/X)$, $Y=1/\sqrt{R^2+X^2}$, then P_s, Q_s, P_c, Q_c can be calculated from following equations:

$$P_c=U_sU_cY\sin(\delta+\alpha)-U_c^2Y\sin\alpha \tag{1}$$

$$Q_{\rm c} = U_{\rm s}U_{\rm c}Y\cos(\delta+\alpha) - U_{\rm c}^2 Y\cos\alpha \qquad (2)$$

$$P_{\rm s} = U_{\rm s}U_{\rm c}Y\sin(\delta-\alpha) + U_{\rm s}^2 Y\sin\alpha \qquad (3)$$

$$Q_{\rm s} = -U_{\rm s}U_{\rm c}Y\cos(\delta-\alpha) + U_{\rm s}^2 Y\cos\alpha \qquad (4)$$

Assume that the DC voltage utilization ratio of PWM equals to1, and the modulation index is m, then $U_{\rm c}$ can be obtained:

$$U_{\rm c} = \frac{m}{\sqrt{2}}U_{\rm d}, \qquad 0\le m\le 1 \qquad (5)$$

Equation (1)~(5) describe the basic relationship of the VSC, where δ and m are the controlling variables and P and Q are the controlled variables.

1.2 Deducing of Mathematical Analysis Expressions for Power Control

$P_{\rm s}$ and $Q_{\rm s}$ are chosen as controlled variables considering that VSC's resistance loss can be neglected.

According to (3) and (4), it is complicated to control the power delivery on account of the influence of the coupling relationship between controlling and controlled variables. To weaken the coupling relationship, the coordinate conversion and variables substitution are adopted.

A and B are defined as

$$\begin{cases} A = U_{\rm c}\cos\delta \\ B = U_{\rm c}\sin\delta \end{cases} \qquad (6)$$

Substituting (6) into (3) and (4) yields

$$P_{\rm s} = U_{\rm s}Y(B\cos\alpha - A\sin\alpha) + U_{\rm s}^2 Y\sin\alpha \qquad (7)$$

$$Q_{\rm s} = -U_{\rm s}Y(A\cos\alpha + B\sin\alpha) + U_{\rm s}^2 Y\cos\alpha \qquad (8)$$

According to (7) and (8), the substitute variable X and Z are defined as

$$X = B\cos\alpha - A\sin\alpha = \frac{P_{\rm s} - U_{\rm s}^2 Y\sin\alpha}{U_{\rm s}Y} \qquad (9)$$

$$Z = A\cos\alpha + B\sin\alpha = \frac{U_{\rm s}^2 Y\cos\alpha - Q_{\rm s}}{U_{\rm s}Y} \qquad (10)$$

Variable A and B can be calculated as follows, based on (9) and (10),

$$A = Z\cos\alpha - X\sin\alpha \qquad (11)$$

$$B = X\cos\alpha + Z\sin\alpha \qquad (12)$$

Variables m and δ are acquired from (6),

$$\delta = \arctan(B/A) \qquad (13)$$

$$m = \sqrt{2}A/(U_{\rm d}\cos\delta) \qquad (14)$$

Equations (9)~(14) are the mathematical expressions for adjusting the active power and reactive power of VSC-HVDC.

1.3 Analysis of Control Strategy Designed

1）Theory study.

It is shown in (9) and (10) that $P_{\rm s}$ is determined by substitute variable X, and $Q_{\rm s}$ is just determined by another substitute variable Z when the system voltage $U_{\rm s}$ is constant. However, both X and Z are relevant to A and B simultaneously.

From (5), (6), and the range of the modulation index m, yields

$$\begin{cases} |A| \le (U_{\rm d}/\sqrt{2}) \\ |B| \le (U_{\rm d}/\sqrt{2}) \\ A^2 + B^2 \le (U_{\rm d}^2/2) \end{cases} \qquad (15)$$

Based on (15), a circle that represents the bound of the variables A and B is shown in Fig.2.

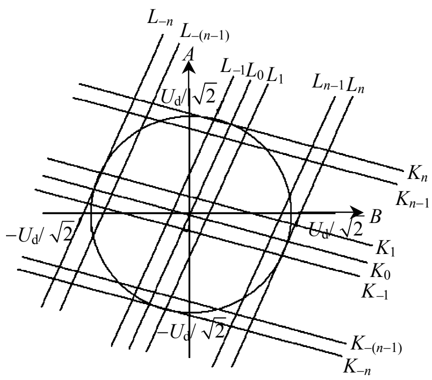

图 2　控制策略的性能示意图

Fig. 2　Characteristic diagram of control strategy

According to (9) and (10), obtain,

$$A = (B/\tan\alpha) - (X/\sin\alpha) \qquad (16)$$

$$A = (Z/\cos\alpha) - B\tan\alpha \qquad (17)$$

Equation (16) represents a series of straight lines named L_i shown in Fig.2 and each line represents the movement track of variable A and B when X is constant. In other words, if A and B change simultaneously along a line (L_i)'s track, X is constant and then $P_{\rm s}$ is determined. However, $Q_{\rm s}$ can be adjusted independently without changing the magnitude of $P_{\rm s}$.

Equation (17) represents a series of straight lines named K_i shown in Fig.2 and each line represents the movement track of variable A and B when Z is constant. If A and B change simultaneously along a line (K_i)'s track, Z is constant and then $Q_{\rm s}$ is determined. However, P_s can be adjusted independently without changing the magnitude of Q_s.

2) Limits deducing for P_s and Q_s.

From the above analysis, the novel control strategy can independently control the active and reactive power. However, it must meet certain condition, i.e. the operation point of A and B must locate in the circle, meaning that K_i and L_i must intersect in the circle shown in Fig.2.

The limits of P_s and Q_s can be obtained and the deducing process is given in Appendix A.

$$P_{smax} = U_d U_s Y / \sqrt{2} + U_s^2 Y \sin\alpha \quad (18)$$

$$P_{smin} = -U_d U_s Y / \sqrt{2} + U_s^2 Y \sin\alpha \quad (19)$$

$$Q_{smax} = U_d U_s Y / \sqrt{2} + U_s^2 Y \cos\alpha \quad (20)$$

$$Q_{smin} = -U_d U_s Y / \sqrt{2} + U_s^2 Y \cos\alpha \quad (21)$$

However, P_s and Q_s are impossible to reach the extreme value simultaneously.

3) Interaction of the controlled variables P_s and Q_s.

Based on the mathematical expressions deduced above and the circle shown in Fig.2, the operation zone of Q_s when P_s is constant can be gotten,

$$U_s^2 Y\cos\alpha - \frac{U_s Y}{2}\sqrt{2U_d^2 - 4\left(\frac{P_s - U_s^2 Y\sin\alpha}{U_s Y}\right)^2} \le Q_s \le U_s^2 Y\cos\alpha + \frac{U_s Y}{2}\sqrt{2U_d^2 - 4\left(\frac{P_s - U_s^2 Y\sin\alpha}{U_s Y}\right)^2} \quad (22)$$

And the operation zone of P_s when Q_s is constant can be expressed as,

$$-\frac{U_s Y}{2}\sqrt{2U_d^2 - 4\left(\frac{U_s^2 Y\cos\alpha - Q_s}{U_s Y}\right)^2} + U_s^2 Y\sin\alpha \le P_s \le \frac{U_s Y}{2}\sqrt{2U_d^2 - 4\left(\frac{U_s^2 Y\cos\alpha - Q_s}{U_s Y}\right)^2} + U_s^2 Y\sin\alpha \quad (23)$$

The deducing process is given in Appendix B.

2 CONTROLLERS DESIGN

2.1 Constant Power Control At Inverter Side

In this paper, two-terminal VSC-HVDC system is shown in Fig.3. At the rectifier side, constant DC voltage control and constant reactive power control are adopted. And constant active and reactive power control, which adopts the control algorithm designed in the paper, is implemented at the inverter side.

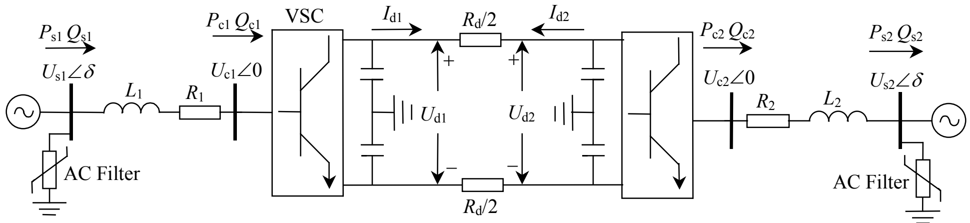

图3 两端VSC-HVDC系统图

Fig. 3 Two-terminal VSC-HVDC system

According to the discussion above, the structure of control system adopting PI controllers and inverse system method are shown in Fig.4.

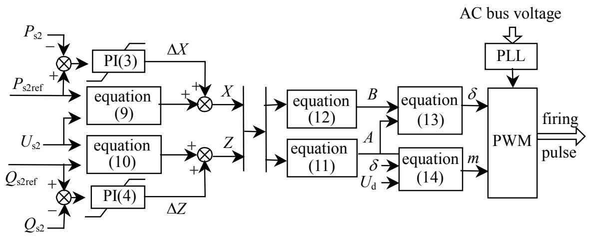

图4 定功率控制系统图

Fig. 4 Constant power control system

2.2 Constant DC Voltage Control at Rectifier Side

DC voltage depends on the storage energy of the capacitor at the DC side. It is necessary to adjust the energy absorbed by VSC to keep the storage energy of the capacitor constant for the invariableness of DC voltage. Assume that Δt is a sampling cycle, and from Fig.1 we can get the energy ΔW absorbed by the capacitor.

$$\Delta W = \frac{1}{4}CU_d^2(t+\Delta t) - \frac{1}{4}CU_d^2(t) = \frac{1}{4}C\Delta[U_d^2(t)] \quad (24)$$

then

$$\Delta[U_d^2(t)] = \frac{4\Delta W}{C} = \frac{4\Delta P_{dc}\Delta t}{C} \quad (25)$$

where ΔP_{dc} is the average power absorbed by the capacitor during the duration of Δt.

According to (25), the change of the square of the DC voltage is proportional to ΔP_{dc}. In a transient course, P_d varies with the DC voltage. Thus, it is necessary to compensate P_d. During the duration of Δt, the resistance of the DC side is almost invariable. Then

$$\frac{U_d(t+\Delta t)}{I_d(t+\Delta t)}=\frac{U_d(t)}{I_d(t)} \tag{26}$$

We know $P_d=U_dI_d$, therefore

$$P_d(t+\Delta t)=\frac{U_d^2(t+\Delta t)}{U_d^2(t)}P_d(t)=(1+\frac{4\Delta P_{dc}\Delta t}{CU_d^2(t)})P_d(t) \tag{27}$$

where $P_d(t+\Delta t)$ is the estimated value of the active power of the DC lines when the DC voltage varies.

According to (27), we can estimate P_d. The control system for constant DC voltage is designed as shown in Fig.5.

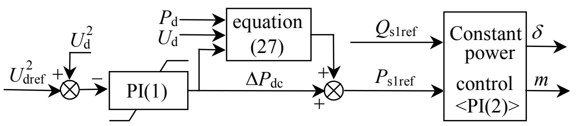

图 5　定直流电压控制系统图

Fig. 5　Control system for constant DC voltage

3　PARAMETERS OPTIMIZATION

3.1　Hooke-Jeeves Algorithm

The Hooke-Jeeves method [20-21] is a numerical solution of nonlinear system.

Assuming an objection function:

$$\min f(x) \tag{28}$$

Equation (28) is called an unconstrained optimization problem. The Hooke-Jeeves method is a direct method for solving problem (28), which only requires f to be continuous. It is employed when f is not differentiable or if the computation of its derivatives is a nontrivial task.

Assume that we are searching for the minimal value of f starting from a given initial base point. The Hooke-Jeeves method computes a new point using the values of f at suitable points along the orthogonal coordinate directions around initial point. The method consists of two steps: an exploration step and an advancing step.

The exploration step proceeds along all the n Cartesian directions, then determine a new base point and a direction for descending value of f. The advancing step goes forward along the direction of the connection of two adjacent base points aiming for decreasing the value of f faster. The exploration step and advancing step compute in turn and find the minimal value of f finally.

3.2　Parameters Optimization

Assume a set of objective for VSC-HVDC system shown in Tab.1.

表 1　VSC-HVDC 系统的控制目标

Tab. 1　Control objectives of VSC-HVDC system

U_{dref}/kV	Q_{s1ref}/Mvar	P_{s2ref}/MW	Q_{s2ref}/Mvar
120	−20	50	40

It can be seen from Fig.4 and Fig.5 that the performance of VSC-HVDC system can be regulated by four sets of PI parameters, i.e. PI(1), PI(2), PI(3) and PI(4). PI(1) and PI(2) are used to control DC voltage and reactive power at rectifier side, and PI(3) and PI(4) are used to control active power and reactive power at inverter side. Because no communication is needed between two sides of VSC-HVDC, PI controllers at rectifier side and inverter side can be adjusted independently. Considering DC voltage control is critical for VSC-HVDC, PI(1) is the most important among four sets of PI controllers. After proper PI parameters are selected, the VSC-HVDC can obtain satisfactory results. In this paper, the proportion in PI parameters is expressed as K and the integral time constant is expressed as T.

For the VSC-HVDC system, the objective function is expressed in (29),

$$f(\boldsymbol{H})=\sum_{j=1}^{4}\omega_j\int_0^T t\left|e_j(t)\right|^2\mathrm{d}t=\sum_{j=1}^{4}\int_0^T t\left|e_j(t)\right|^2\mathrm{d}t \tag{29}$$

where: $e_j(t)$ is the error between the No.j real value of the controlled variable and its desired value; ω_j is weight, considered to be 1 in the paper; Vector $\boldsymbol{H}$= [k_1 T_1 k_2 T_2 k_3 T_3 k_4 T_4] are the variables. The corresponding flow chart is represented in Fig.6.

For Hooke-Jeeves algorithm, initial parameters should be selected. Also initial step size and step reduction factor, which are set to 0.01 and 1.2 respectively in this paper. Tab.2 shows the initial and optimized control system parameters as well as

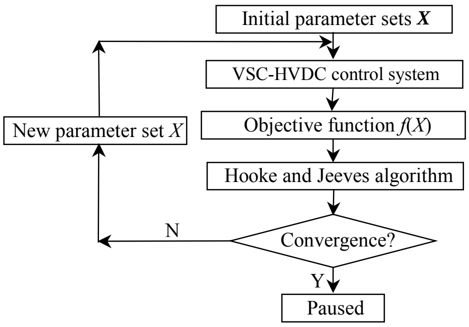

图 6 VSC-HVDC 控制系统参数优化流程图

Fig. 6 Flow chart of VSC-HVDC control system parameters optimization

表 2 优化前后控制参数及目标方程值的比较

Tab. 2 Comparison between initial and optimized parameters and objective function value

Parameters	Initial	Optimized
K_1	0.223	0.173
T_1	0.043	0.073
K_2	0.356	0.356
T_2	0.034	0.014
K_3	0.723	0.683
T_3	0.132	0.102
K_4	0.522	0.582
T_4	0.036	0.054
$f(X)$	291.760	14.470

the corresponding objective function values.

4 SIMULATION RESEARCH

4.1 Operation Performance Comparison Between Systems With Initial and Optimized Parameters

Based on the two-terminal VSC-HVDC structure shown in Fig.3, operation performance comparison of steady state between systems with initial and optimized parameters is shown in Fig.7~ Fig.10.

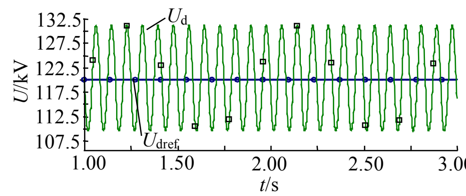

(a) DC voltage results with initial parameters

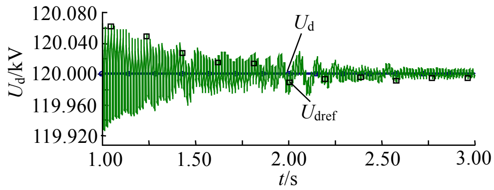

(b) DC voltage results with optimized parameters

图 7 整流侧直流电压优化前后的比较

Fig. 7 DC voltage comparison at rectifier side

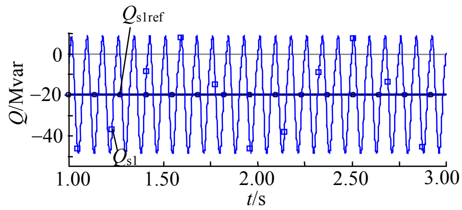

(a) Reactive power results with initial parameters

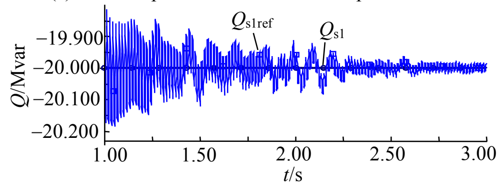

(b) Reactive power results with optimized parameters

图 8 整流侧无功功率优化前后的比较

Fig. 8 Reactive power comparison at rectifier side

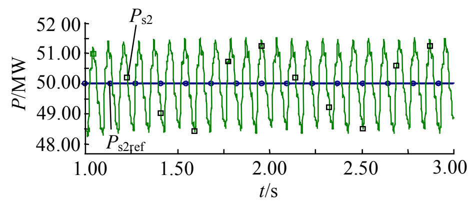

(a) Active power results with initial parameters

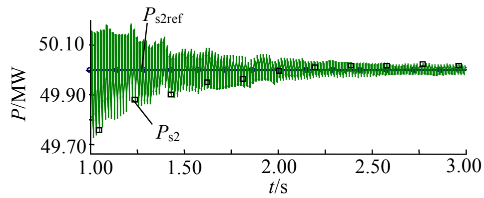

(b) Active power results with optimized parameters

图 9 逆变侧有功功率优化前后的比较

Fig. 9 Active power comparison at inverter side

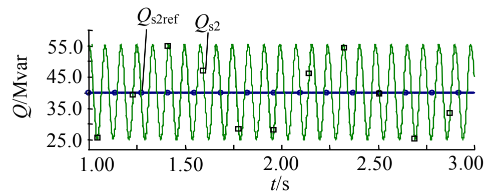

(a) Reactive power results with initial parameters

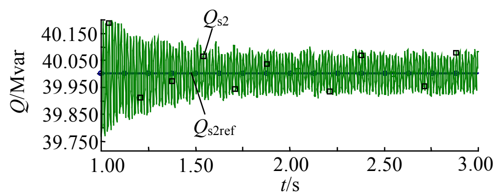

(b) Reactive power results with optimized parameters

图 10 逆变侧无功功率优化前后的比较

Fig. 10 Reactive power comparison at inverter side

It is noted that because the start-up process of VSC-HVDC, which is reflected by transient process in Fig.7~Fig.10, is beyond the scope of this paper, only simulation results after 1.0 s have been shown.

The parameters of tested system are as follow:

The rated AC voltage at rectifier side is 13.8 kV, the transformer ratio is 13.8 kV/62.5 kV; the rated AC voltage at inverter side is 115 kV, the transformer ratio is 62.5 kV/115 kV. The equivalent loss resistances of commuting transformer at both sides are 0.1 Ω, and the equivalent L is 0.25 mH. The capacitance C of both sides is 500 μF. The equivalent resistance R_d of transmission line is 5 Ω. The DC voltage is 120 kV.

It is noted that the variable with subscript of “ref” is the reference value in each simulation figure, and the other variable is the real value. For example, the variable U_{dref} is the DC voltage reference value and U_d is the real value.

Tab.3 shows the maximum error percentage comparison between initial and optimized control performance.

表 3　优化前后控制目标最大误差百分比的比较

Tab. 3　Maximum error percentage comparison between initial and optimized control performance

Parameters	e_{ini}/%	e_{opt}/%
U_d	10.4	0.067
Q_{s1}	150	1
P_{s2}	4	0.6
Q_{s2}	37.5	0.5

From the simulation results and Tab.3, it can be observed that the system performance with optimized parameters has been greatly improved, especially, the maximum error percentage of U_d decreases by 155 times. In fact, the genetic algorithm in [16] and simplex algorithm in [17] also show the improved performances. However, quantified indexes have not been presented in them. Compared with simplex algorithm, Hooke-Jeeves algorithm is a more flexible arithmetic due to its changeable step reduction factor; and the optimization process of Hooke-Jeeves algorithm is simple compared with the complex coding and optimization steps of genetic algorithm. The main shortcoming of Hooke-Jeeves algorithm is its local optimization characteristic. However, any optimization algorithms must be supplied with initial values. Once initial values, which can stabilize the system approximately, are supplied, optimization solutions can be found around them using Hooke-Jeeves algorithm. Therefore, the problem mentioned above can be solved.

4.2　Dynamic Operation Performance

To prove the availability of control strategy, the researches about the power step-change and DC voltage lifting-up are simulated using PSCAD/EMTDC.

With the optimized parameters, dynamic operation performance is studied to testify the robustness of the controllers.

Case 1: Power step-change.

Case is as follows: simulation process lasts 5 s, the active power P_{s2} changes from 50 MW to 30 MW at 3 s and the reactive power Q_{s2} changes from 40 Mvar to 60 Mvar at 4 s. Simulation results are shown in Fig.11~Fig.13.

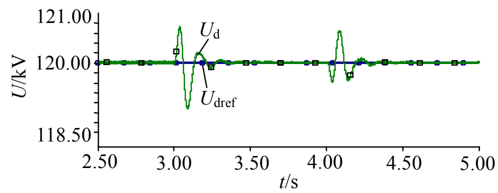

图 11　整流侧直流电压

Fig. 11　DC voltage at rectifier side

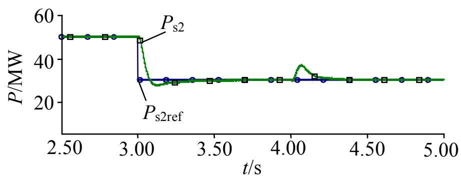

图 12　逆变侧有功功率

Fig. 12　Active power at inverter side

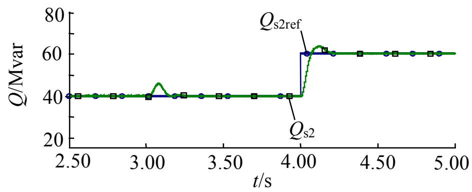

图 13　逆变侧无功功率

Fig. 13　Reactive power at inverter side

The simulation results show that the maximum dynamic error of DC voltage is 8.3%. When the reference value of either active or reactive power happens to step change, it can reach the pre-set value instantly. The other variable has slight fluctuation during the adjusting period, and then maintains initial value. Therefore, it can realize the independent control of the active and reactive power. It can be concluded that the controller designed is feasible and the parameters optimization algorithm is effective.

Active and reactive power influence each other. However, the whole system achieves stable state within about 1 s after power step-change. Simulation results clearly show that the system performance is stable under the case 1 condition.

Case 2: DC voltage lifting-up.

When t=3.0 s, the DC voltage is lifted up by 4.2%. The simulation results of DC voltage lifting-up are described in Fig.14 and Fig.15.

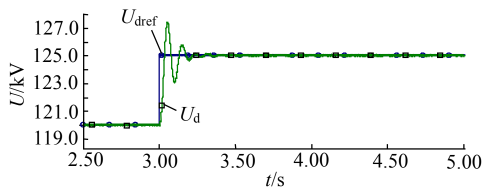

图 14 整流侧直流电压

Fig. 14 DC voltage at rectifier side

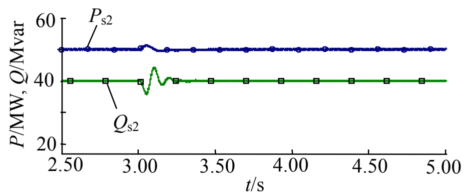

图 15 逆变侧有功功率和无功功率

Fig. 15 Active and reactive power at inverter side

In Fig.14, the overshoot of U_d is 2.08%, and the settle time is 0.26 s. It is shown in Fig.15 that active and reactive power has slight fluctuation during DC voltage lift-up. Although DC voltage at rectifier side is lifted up, active and reactive power at inverter side can be maintained at initial values; and it can be proved that the controllers at rectifier side and inverter side can be adjusted independently. From the results, it is concluded that the proposed control strategy with optimized parameters can provide a stable operation and fast response under DC voltage lifting-up circumstance.

5 CONCLUSIONS

1）The control strategy proposed is able to control the active and reactive power independently.

2）The Hooke-Jeeves optimization algorithm can be adopted to optimize the PI parameters, and system performance can be greatly improved.

3）With the support of optimized parameters, the controllers will have high response speed, desirable stability and greatly improved dynamic performances.

4）Robustness of the controllers is proved, when system operates at different points under the conditions of power step-change and DC voltage lift-up.

REFERENCES

[1] 徐政．交直流电力系统动态行为分析[M]．北京：机械工业出版社，2004：12-13．
Xu Zheng．Dynamic behavior analysis of AC-DC power system [M]．Beijing：China Machine Press，2004：12-13(in Chinese)．

[2] Asplund G，Eriksson K，Tollerz O．HVDC light: a tool for electric power transmission to distant loads[C]．VI Sepope Conference，Salvador，Brazil，1998．

[3] Weimers L．New markets need new technology[C]．International Conference on Power System Technology，Perth，Australia，2000．

[4] Reed G，Pape R，Takeda M. Advantages of voltage sourced converter (VSC) based design concepts for FACTS and HVDC-link applications[C]．IEEE Power Engineering Society General Meeting，Toronto，Canada，2003．

[5] Stendius L，Eriksson K. HVDC light：an excellent tool for city center infeed[C]．Power Generation Conference，Singapore，1999．

[6] Meshram P M，Kadu A N，Nagpure R N，et al．VSC-HVDC for improvement of quality of power supply[C]．IEEE Region 10 Conference，Nagpur，India，2004．

[7] Zhang Guibin，Xu Zheng，Liu Hongtao．Supply passive networks with VSC-HVDC[C]．2001 Power Engineering Society Summer Meeting，Hangzhou，China，2001．

[8] 胡兆庆，毛承雄，陆继明，等．一种新型的直流输电技术 HVDC：Light[J]．电工技术学报，2005，20(7)：12-16．
Hu Zhaoqing，Mao Chengxiong，Lu Jiming，et al．A new HVDC technology HVDC-light[J]．Transactions of China Electrotechnical Society，2005，20(7)：12-16(in Chinese)．

[9] 李庚银，吕鹏飞，李广凯，等．轻型高压直流输电技术的发展与展望[J]．电力系统自动化，2003，27(4)：77-81．
Li Gengyin，Lü Pengfei，Li Guangkai，et al．Development and prospects for HVDC light[J]．Automation of Electric Power Systems，2003，27(4)：77-81(in Chinese)．

[10] 张桂斌，徐政，王广柱．基于 VSC 的直流输电系统的稳态建模及其非线性控制[J]．中国电机工程学报，2002，22(1)：17-22．
Zhang Guibin，Xu Zheng，Wang Guangzhu．Steady-state model and its nonlinear control of VSC-HVDC system[J]．Proceedings of the CSEE，2002，22(1)：17-22(in Chinese)．

[11] 陈谦，唐国庆，胡铭．采用 dq0 坐标的 VSC-HVDC 稳态模型与控制器设计[J]．电力系统自动化，2004，28(16)：61-66．
Chen Qian，Tang Guoqing，Hu Ming．Steady-state model and controller design of a VSC-HVDC converter based on dq0-axis [J]．Automation of Electric Power Systems，2004，28(16)：61-66(in Chinese)．

[12] 赵成勇，李金丰，李广凯．基于有功和无功独立调节的VSC-HVDC控制策略[J]．电力系统自动化，2005，29(9)：20-24．

Zhao Chengyong，Li Jinfeng，Li Guangkai．VSC-HVDC control strategy based on respectively adjustment of active and reactive power[J]．Automation of Electric Power Systems，2005，29(9)：20-24(in Chinese)．

[13] Li Gengyin，Yin Ming，Zhou Ming，et al．Modeling of VSC-HVDC and control strategies for supplying both active and passive systems[C]．Power Engineering Society General Meeting，Montreal，Canada，2006．

[14] Padiyar K R，Prabhu N．Modelling control design and analysis of VSC based HVDC transmission systems[C]．2004 International Conference on Power System Technology，Singapore，2004．

[15] 陈海荣，徐政．基于同步坐标变换的 VSC-HVDC 暂态模型及其控制器[J]．电工技术学报，2007，22(2)：121-126．
Chen Hairong，Xu Zheng．Transient model and controller design for VSC-HVDC based on synchronous reference frame[J]．Transactions of China Electrotechnical Society，2007，22(2)：121-126(in Chinese)．

[16] 陈蔓，陆继明，毛承雄，等．基于遗传算法的优化控制在 VSC-HVDC 中的应用[J]. 电力系统及其自动化学报，2006，18(4)：19-23．
Chen Man，Lu Jiming，Mao Chengxiong，et al．Application of genetic algorithm based optimal control in VSC-HVDC [J]. Proceedings of the CSU-EPSA，2006，18(4)：19-23(in Chinese)．

[17] Zhao Chengyong，Lu Xiangdong，Li Guangkai．Parameters optimization of VSC-HVDC control system based on simplex algorithm[C]. Power Engineering Society General Meeting，Tampa，Florida，2007．

[18] 胡兆庆，毛承雄，陆继明．一种优化控制策略在基于电压源换流器的 HVDC 系统中的应用[J]．电网技术，2004，28(10)：38-41．
Hu Zhaoqing，Mao Chengxiong，Lu Jiming．Application of an optimal control strategy to a new type of HVDC system based on voltage source converter[J]．Power System Technology，2004，28(10)：38-41(in Chinese)．

[19] 李金丰．轻型直流输电控制策略及控制系统软件设计[D]．保定：华北电力大学，2004．
Li Jinfeng．Control strategy for VSC-HVDC and design of control system software[D]. Baoding：North China Electric University，2004 (in Chinese)．

[20] Quarteroni A，Sacco R，Saleri F．Numerical mathematics [M]．Beijing：Science Press，2006：301-302．

[21] 陈宝林．最优化理论与算法[M]．北京：清华大学出版社，1989：301-302．
Chen Baolin．Optimization theory and algorithm[M]．Beijing：Tsinghua University Press，1989：301-302(in Chinese)．

APPENDIX A

From (15) and (16), obtain

$$|X| \le U_{\mathrm{d}}/\sqrt{2} \tag{A1}$$

When $A=-U_{\mathrm{d}}\sin\alpha/\sqrt{2}$, $B=U_{\mathrm{d}}\cos\alpha/\sqrt{2}$, and $X_{\max}=U_{\mathrm{d}}/\sqrt{2}$ are met,

$$P_{\mathrm{smax}}=U_{\mathrm{d}}U_{\mathrm{s}}Y/\sqrt{2}+U_{\mathrm{s}}^{2}Y\sin\alpha \tag{A2}$$

When $A=U_{\mathrm{d}}\sin\alpha/\sqrt{2}$, $B=-U_{\mathrm{d}}\cos\alpha/\sqrt{2}$, and $X_{\min}=-U_{\mathrm{d}}/\sqrt{2}$ are met,

$$P_{\mathrm{smin}}=-U_{\mathrm{d}}U_{\mathrm{s}}Y/\sqrt{2}+U_{\mathrm{s}}^{2}Y\sin\alpha \tag{A3}$$

Similarly, from (15) and (17), obtain

$$|Z| \le U_{\mathrm{d}}/\sqrt{2} \tag{A4}$$

When $A=-U_{\mathrm{d}}\cos\alpha/\sqrt{2}$, $B=-U_{\mathrm{d}}\sin\alpha/\sqrt{2}$ and $Z_{\min}=-U_{\mathrm{d}}/\sqrt{2}$ are met,

$$Q_{\mathrm{smax}}=U_{\mathrm{d}}U_{\mathrm{s}}Y/\sqrt{2}+U_{\mathrm{s}}^{2}Y\cos\alpha \tag{A5}$$

When $A=U_{\mathrm{d}}\cos\alpha/\sqrt{2}$, $B=U_{\mathrm{d}}\sin\alpha/\sqrt{2}$ and $Z_{\max}=U_{\mathrm{d}}/\sqrt{2}$ are met,

$$Q_{\mathrm{smin}}=-U_{\mathrm{d}}U_{\mathrm{s}}Y/\sqrt{2}+U_{\mathrm{s}}^{2}Y\cos\alpha \tag{A6}$$

APPENDIX B

The range of variable Z is derived as,

$$-\frac{1}{2}\sqrt{2U_{\mathrm{d}}^{2}-4X^{2}} \le Z \le \frac{1}{2}\sqrt{2U_{\mathrm{d}}^{2}-4X^{2}} \tag{B1}$$

According to (10), obtain,

$$U_{\mathrm{s}}^{2}Y\cos\alpha-\frac{U_{\mathrm{s}}Y}{2}\sqrt{2U_{\mathrm{d}}^{2}-4X^{2}} \le Q_{\mathrm{s}} \le U_{\mathrm{s}}^{2}Y\cos\alpha+\frac{U_{\mathrm{s}}Y}{2}\sqrt{2U_{\mathrm{d}}^{2}-4X^{2}} \tag{B2}$$

Substituting (9) into (A4), obtain the operation zone of Q_{s} when P_{s} is constant,

$$U_{\mathrm{s}}^{2}Y\cos\alpha-\frac{U_{\mathrm{s}}Y}{2}\sqrt{2U_{\mathrm{d}}^{2}-4\left(\frac{P_{\mathrm{s}}-U_{\mathrm{s}}^{2}Y\sin\alpha}{U_{\mathrm{s}}Y}\right)^{2}} \le Q_{\mathrm{s}} \le U_{\mathrm{s}}^{2}Y\cos\alpha+\frac{U_{\mathrm{s}}Y}{2}\sqrt{2U_{\mathrm{d}}^{2}-4\left(\frac{P_{\mathrm{s}}-U_{\mathrm{s}}^{2}Y\sin\alpha}{U_{\mathrm{s}}Y}\right)^{2}} \tag{B3}$$

With the same method, the operation zone of P_{s} when Q_{s} is constant is expressed as,

$$-\frac{U_{\mathrm{s}}Y}{2}\sqrt{2U_{\mathrm{d}}^{2}-4\left(\frac{U_{\mathrm{s}}^{2}Y\cos\alpha-Q_{\mathrm{s}}}{U_{\mathrm{s}}Y}\right)^{2}}+U_{\mathrm{s}}^{2}Y\sin\alpha \le P_{\mathrm{s}} \le \frac{U_{\mathrm{s}}Y}{2}\sqrt{2U_{\mathrm{d}}^{2}-4\left(\frac{U_{\mathrm{s}}^{2}Y\cos\alpha-Q_{\mathrm{s}}}{U_{\mathrm{s}}Y}\right)^{2}}+U_{\mathrm{s}}^{2}Y\sin\alpha \tag{B4}$$

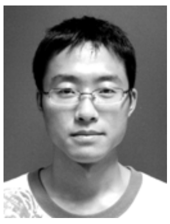

郭春义

收稿日期：2009-02-01。

作者简介：

郭春义(1984—)，男，博士研究生，研究方向为高压直流输电技术，freesky_guo@163.com；

赵成勇(1964—)，男，博士，教授，博士生导师，主要研究方向为直流输电、电能质量分析与控制等，chengyongzhao@ncepu.edu.cn。

(责任编辑　刘浩芳)